

SOLAR CORONA, SOLAR WIND STRUCTURE AND SOLAR PARTICLE EVENTS

Volker Bothmer

Extraterrestrische Physik, Universität Kiel, Kiel, Germany

ABSTRACT

This paper presents a brief overview on the current understanding of the structure of the Sun's atmosphere, its extension into the interplanetary medium, its temporal changes and the solar sources of terrestrial effects, such as magnetospheric storms, power outages or solar radiation hazards. The overview is based on new observations from Yohkoh, Ulysses, SOHO (Solar and Heliospheric Observatory) and other recent space missions which are now dramatically enhancing the scientific knowledge in solar and heliospheric physics and that of the Sun-Earth connection theme in general. The new measurements of in situ particle, plasma and magnetic field parameters, and optical (EUV, X-ray, white-light) observations have led to a new understanding of the major phenomena that control space weather. This progress will be continued through NASA's planned STEREO (Solar TERrestrial Relations Observatory) mission, to be launched in 2004, that will establish besides major breakthroughs in solar/heliospheric physics, the first real time space weather predictions.

Key words: solar corona; solar wind; coronal mass ejections; solar energetic particles; space weather.

1. INTRODUCTION

The Earth is not surrounded by totally empty space, but, like the other planets of the solar system, it is continuously embedded in a stream of ionised particles, the so called solar wind, emanating from the Sun's hot outer atmosphere. At a distance of about 150 Million kilometres (1 AU) from the Sun, this supersonic plasma flow permanently blows past the outer terrestrial magnetic field. The solar wind compresses the Earth's magnetic field at the dayside magnetosphere and stretches it out deeply into interplanetary space at the nightside. With respect to the Earth's magnetosphere, the solar wind induces a conductive electric field, $\underline{E} = -\underline{v} \times \underline{B}$. This electric field changes in magnitude when the parameters of the solar wind change due to variations of the solar magnetic field. The Sun's changing magnetic field is "directly" visible in Figure 1, which shows variations of the intensity of the Sun's X-ray corona during the period 1991-1995. It is also well known now, that it is not simply the enhanced electric field magnitude that enhances the energy transfer into the magnetosphere, but that the direction of the

interplanetary magnetic field (IMF) is of crucial importance. When the IMF, which is carried out from the Sun by the solar wind, is directed anti-parallel to the Earth's dayside field, efficient magnetic coupling is stimulated (Russell & McPherron 1973, Tsurutani et al. 1988, Tsurutani et al. 1992, Bothmer & Schwenn 1995).

In situ measurements of the solar wind, by satellites that left the Earth's magnetosphere during parts of its' orbits, have provided direct evidence that this plasma flow is not homogenous, but that it can change from a mild breeze to a hurricane rapidly (Hirshberg et al. 1972, Gosling et al. 1973). Such solar wind disturbances have been unambiguously identified as sources of, amongst other hazards, satellite failures, power outages and telecommunication problems (Allen et al. 1989, Gorney 1990, Shea et al. 1992, Lanzerotti et al. 1997). During the onsets of powerful solar eruptions, particles can be accelerated up to hundreds of MeV or sometimes even to GeV energies which pose severe danger to astronauts (Foundations of solar particle event risk management, Anser, Arlington, VA 22202, USA). Electrons at keV energies can bury themselves into spacecraft electronic systems, later often producing deep dielectric discharging events that may lead to complete losses of devices and even of whole spacecraft (Baker et al. 1998). Additionally to the solar wind and suprathermal particle flows, a permanent stream of energetic particles at considerable higher energies ($\gg 100$ MeV/n) continuously penetrates into the heliosphere from the interstellar medium. These particles are much less in intensity, but due to their high energies, they can cause electronic damages of satellite systems (Lanzerotti et al. 1997).

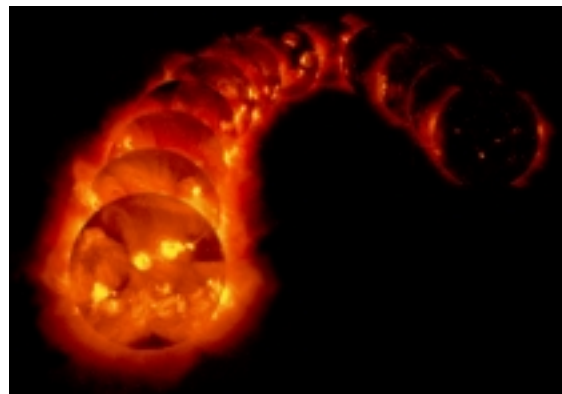


Figure 1. The variability of the Sun's X-ray corona between 1991-1995. Each image was taken 120 days apart. Courtesy Yohkoh/SXT consortium.

It is certainly interesting to note, that a SEU (single event upset) caused a malfunction of the SOHO (Solar and Heliospheric Observatory) star tracker during the final work on this manuscript. The star tracker is SOHO's main navigation tool since the last of the three on board gyros failed to work properly (<http://soho.wwwww.estec.esa.nl>).

The solar wind, the energetic particle and cosmic ray intensity varies in the course of the about eleven year solar cycle. At times of high solar activity, solar wind "thunderstorms" and solar energetic particle events ("particle blizzards") are most frequent and powerful, whereas the cosmic ray intensity is at a minimum. The high solar activity complicates particle entry into the inner heliosphere, whereas at times of minimum activity, when the solar wind is less stormy and the solar magnetic field remains for some time in a quasi steady-state, cosmic rays can penetrate the heliosphere most easily (e.g., McKibben et al. 1995).

There are also other forms of matter present in near Earth's orbit, e.g., interstellar dust, which I do not consider in more detail in the present paper. Further, there always exists a certain level of danger of possible bombardments through minor celestial bodies (e.g., the impact of the fragments of comet Shoemaker-Levy on Jupiter). However, I would call such event a natural catastrophe rather than a space weather ingredient. Thus, it is the varying activity of the Sun, that is reflected in variations of the solar wind (which includes the IMF) and suprathermal particle flows, that determines space weather conditions. Note that the definition of the prime ingredients is depending on the radial distance with respect to the Sun and that effects of solar irradiance variations on Earth are not addressed in this overview.

In the following sections I will try to give a brief summary on the current understanding of the origin, structure and variations of the solar wind that controls the geospace system and the solar origin of energetic particle events.

2. CORONA AND SOLAR WIND

Since the advent of the space age, satellite measurements outside the Earth's magnetosphere have provided detailed measurements of the interplanetary medium. The Helios and Voyager spaceprobes have provided in situ observations of the solar wind as close to the Sun as 0.3 AU and as far off as > 50 AU, and recently the Ulysses spacecraft has explored the full range of heliographic latitudes (Figure 2). The main characteristics of the solar wind measured by satellites in near Earth's orbit are summarized in Table 1. From the characteristics of the in situ measurements, the solar

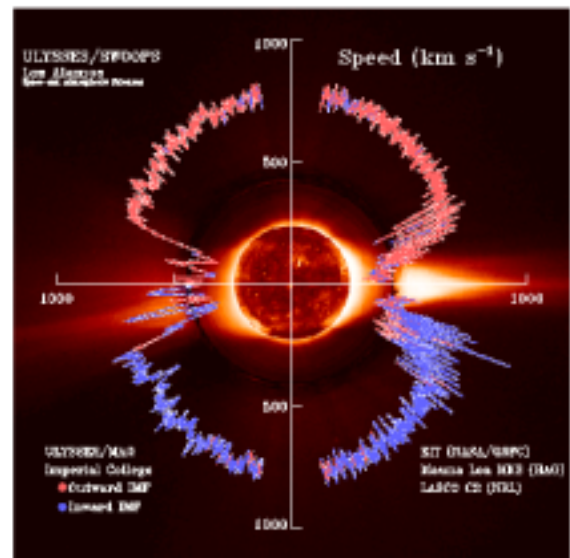


Figure 2. Ulysses observations of the solar wind in the 3-D heliosphere (McComas et al. 1998).

wind may be basically classified into three different types: slow, fast and transient streams (Schwenn 1990). This classification is of course an oversimplification, e.g., the slow solar wind seems to be comprised of different types itself (Wang 1994).

Observations of the corona at extreme ultraviolet (EUV) wavelengths, e.g., with Skylab (Eddy 1979), have brought direct evidence for the assumption, that coronal holes, where the magnetic field lines are open to interplanetary space, are the sources of the fast solar wind. This view has been confirmed by the Ulysses spacecraft (Figure 2), which for the first time, passed over the Sun's poles (at a radial distance > 1 AU) and performed the first 3-D exploration of the heliosphere

Table 1. Solar wind characteristics near Earth's orbit. Adapted from Schwenn 1990.

Fast Wind	Slow Wind
➤ > 400 km/s	< 400 km/s
➤ $n_p \sim 3 \text{ cm}^{-3}$	$n_p \sim 8 \text{ cm}^{-3}$
➤ ~ 95% H, 4% He, minor ions	~ 94% H, ~ 5% He, minor ions, great variability
➤ $B \sim 5 \text{ nT}$	$B < 5 \text{ nT}$
➤ Alfvénic Fluctuations	Density Fluctuations
➤ Origin in Coronal Holes	Origin 'Above' Coronal Streamers
Transient Wind	
➤ ~ 300 - > 2000 km/s	
➤ Sometimes up to ~ 30% He, sometimes Fe^{+16} , He^+	
➤ Frequently associated with interplanetary shocks	
➤ Origin in Coronal Mass Ejections	

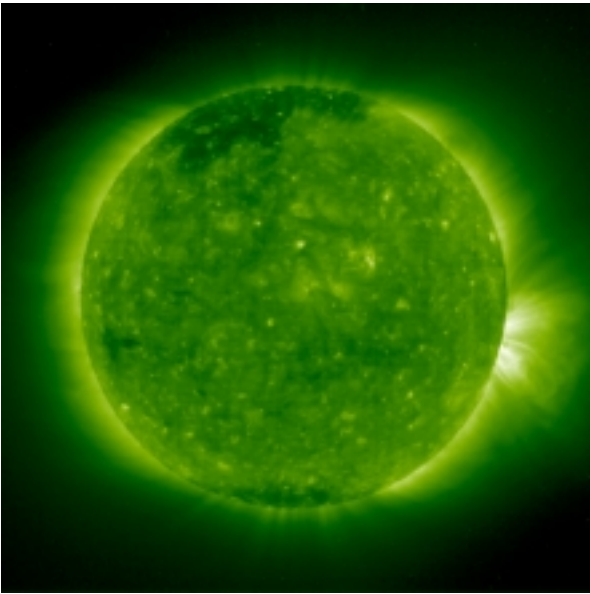


Figure 3. EUV image of the solar corona taken by SOHO/ EIT on September 9, 1996. Courtesy SOHO/ EIT consortium.

(Marsden & Smith 1997). Figure 2 shows that the IMF had outward magnetic polarity in the northern and inward polarity in the southern hemisphere. The difference in the solar wind characteristics between the observations that were taken at low latitudes before the south polar pass (1990-1994, lower right side) and the fast latitude scan after the polar pass (left side) reflect differences in solar activity and differences in the coronal and subsequent solar wind stream structure. Note the recurrent episodes of fast and slow wind streams yielding in an alternating speed pattern before Ulysses passed the south polar regions. The interaction of quasi-stationary fast and slow streams leads to 3-D corotating interaction regions (CIRs) in the heliosphere (e.g., Gosling et al. 1995). Due to the enhanced magnetic field strength, the presence of meridional field deflections and the rising wind speed within in the compression regions, CIRs are well known causes of geomagnetic storms (e.g., Crooker et al. 1996). However, the magnitude in these storms commonly does not exceed Kp-values of 7+ (Bothmer & Schwenn 1995).

Figure 3 shows an image of the corona at 195 Å taken by the Extreme Ultraviolet Telescope (EIT) on board SOHO in September 1996. Large coronal holes at the Sun's north and south poles, typically for solar minimum conditions, dominate the Sun's atmospheric structure. Often these holes have "narrow" extensions to lower latitudes, sometimes even crossing the heliographic equator. Such an extension can be seen in the EUV image shown in Figure 4 which was taken by SOHO/EIT about half a rotation (~ 13.5 days) earlier.

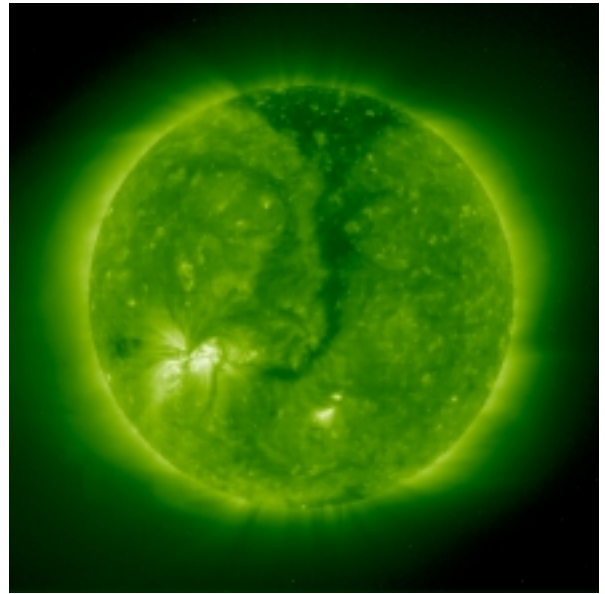


Figure 4. EUV image of the solar corona taken by SOHO/ EIT on August 16, 1996. Courtesy SOHO/ EIT consortium.

The extension of the northern coronal hole, termed "Elephant's Trunk", lasted for at least two rotations (Bromage et al. 1997). Such extensions can persist over many rotations (e.g., the "Italian Boot", see Eddy 1979). As a consequence of this coronal hole extension, fast solar wind was observed by the WIND spacecraft near Earth's orbit (A.J. Lazarus, priv. communications).

However, solar wind from coronal holes is not observed only if a heliospheric observer is positioned at the heliographic latitudes of the coronal holes itself. Ulysses was already immersed in fast wind from coronal holes at times when the spacecraft was at ~ 40° heliographic latitude, whereas the coronal hole boundaries were located at ~ 60° (Gosling et al. 1995).

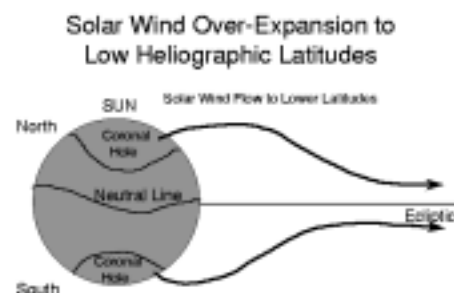


Figure 5. Sketch of non-radial expansion of fast solar wind from polar coronal holes into the ecliptic.

This observation supports non-radial expansion models of solar wind streams from high latitude coronal holes down to equatorial latitudes (Wang et al. 1996) and a dependence of solar wind speed on expansion of coronal magnetic flux-tubes. The non-radial expansion is expected to take place close to the Sun, within radial distances of about three solar radii from the photosphere (Wang et al. 1997). It seems likely, that at least during solar minimum, most of the solar wind in the heliosphere stems from coronal holes where the magnetic field is open to interplanetary space, and that only a minor fraction of the solar wind is due to sporadic plasma releases above coronal streamers (Wang et al. 1998) and in coronal mass ejections (CMEs) which will be described in more detail in section 4.

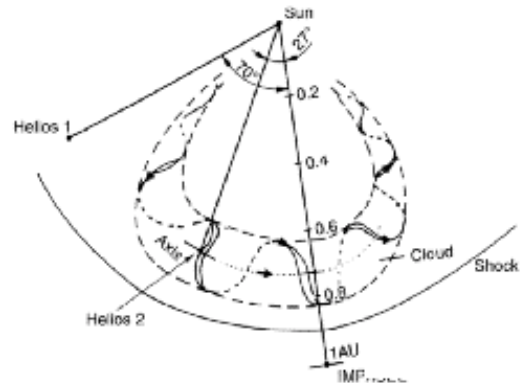


Figure 7. Idealized view of a large-scale magnetic flux-rope in the interplanetary medium (Bothmer & Schwenn 1998).

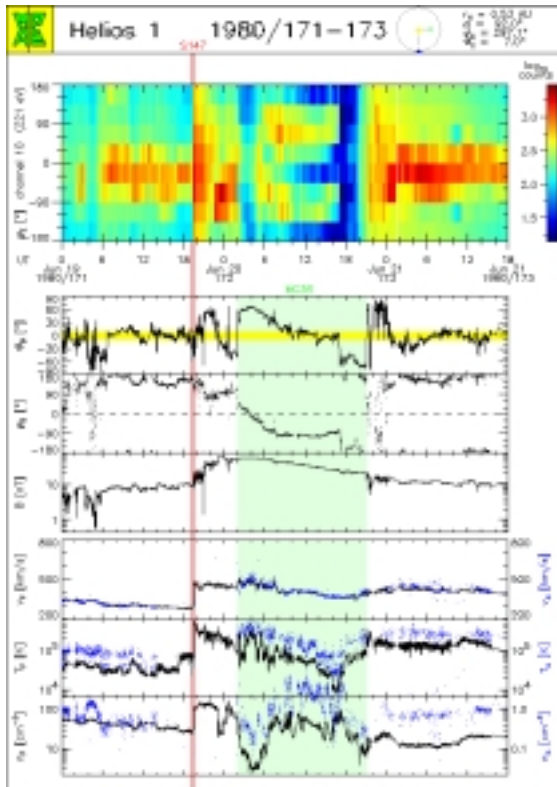


Figure 6. A transient solar wind stream (a flux-rope CME) observed by Helios 1 in 1980, at 0.5 AU. Parameters from top to bottom: Suprathermal electron distribution with energies of 221 eV in 8 bins in the ecliptic, the log of the measured counts within 8° of the ecliptic is color-coded; polar, η , and azimuthal, ν , angles of the magnetic field in GSE coordinates; magnetic field strength and proton speed, temperature and density; dotted curves represent the ∇ -particle measurements. The solid line marks the associated interplanetary shock, the shaded region indicates the transient stream. Courtesy K. Ivory, Max-Planck-Institut für Aeronomie.

A non-radial expansion of the solar wind has important implications for the structure of the IMF, e.g., an in-ecliptic observer can become in this way magnetically connected to high solar latitudes as sketched in Figure 5. This and other effects have been described in a recent model by Fisk (1996).

3. TRANSIENT SOLAR WIND

Besides quasi-stationary solar wind streams, the interplanetary medium often exhibits disturbed conditions in form of transient interplanetary shocks, unusual plasma flows, and magnetic field variations

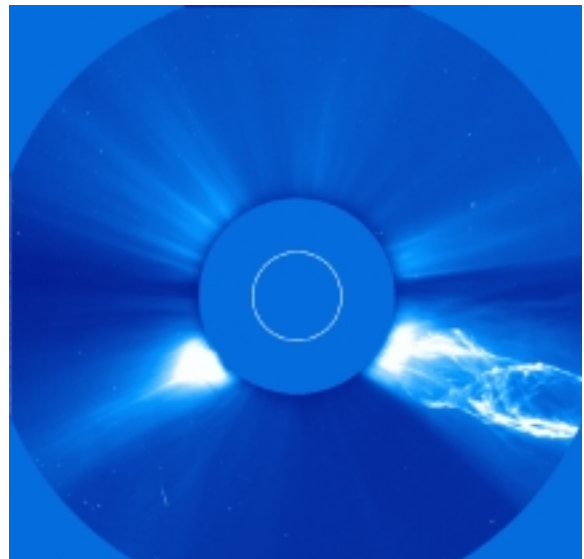


Figure 8. Helical magnetic field structure observed in a prominence eruption. The image was taken by SOHO/LASCO on June 2, 1998. The white circle represents the solar limb. The field of view is 2 to 6 R_s . Courtesy SOHO/LASCO consortium.




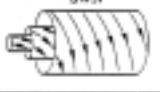




Polarity and Orientation of the Filament	Flux Rope Type
	SEN 
	SWN 
	NES 
	NWS 

Figure 9. Inferred magnetic structure at filament sites in the Sun's southern (right-handed magnetic helicity: SWN, NES) and northern (left-handed magnetic helicity: SEN, NWS) hemispheres, and that of associated transient solar wind streams with helical internal flux-rope structure (Bothmer & Schwenn 1994, 1998).

(e.g., Gosling 1990). Figure 6 shows an example for an unusual solar wind stream, observed by the Helios 1 spacecraft in 1980 at 0.5 AU, that was driving an interplanetary shock wave due to its higher speed than the ambient solar wind ahead. A couple of hours after the shock ($\sim 19:30$ UT on June 19), at about 02:00 UT on June 20, bidirectional streaming of 221 eV suprathermal electrons was observed in coincidence with a large coherent rotation of the magnetic field polar angle, η , from north to south, higher than average magnetic field strength, low ($\ll 1$) plasma- β and a number of other peculiar plasma and field characteristics, lasting until about 21:00 UT on the same day (Bothmer & Schwenn 1998, Burlaga et al. 1982). This transient solar wind stream passed Helios directly as a consequence of a spacecraft-directed CME, detected with the Solwind coronagraph on board the P78/1 satellite (Burlaga et al. 1982). The correlated in situ and optical observations have provided for the first time direct evidence that transient interplanetary shocks in the interplanetary medium are caused by fast CMEs rather than by solar flares (Sheeley et al. 1985). The internal magnetic structure of these streams has been successfully described through MHD-models for force-free magnetic flux-tubes (e.g., Bothmer & Schwenn 1998), as sketched in Figure 7.

Bothmer & Schwenn (1994, 1998) found, that large-scale transient flows with helical internal magnetic field structure (magnetic clouds) can be classified by four different flux-rope types, and that the origin of such flows can be traced back to the Sun to the site of large

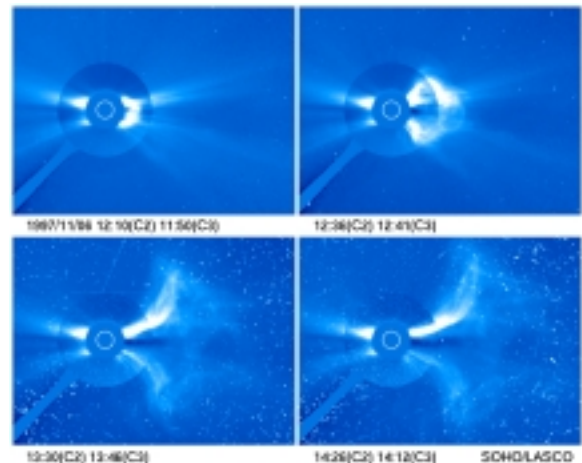


Figure 10. A CME observed by SOHO/LASCO on November 6, 1997 at the west-limb of the Sun. The Sun's limb corresponds to the white circle and the field of view is 2 to 30 R_{\odot} . The CME had a speed of ~ 1600 km/s. Courtesy SOHO/LASCO consortium.

disappearing filaments (erupting prominences) which erupted with CMEs. An example of a CME-associated prominence eruption is shown in Figure 8. Moreover, the analysis yielded an agreement between the in situ observed magnetic flux-rope structure of the transient solar wind flows with that inferred from the magnetic field structures at the sites of the filaments (Figure 9). This result, which was further supported by an extended study of Bothmer & Rust (1997), has important implications for the prediction of geo-effective solar disturbances through detection of earthward directed CMEs and simultaneous solar magnetic field measurements. Such measurements will be provided with unprecedented quality by the planned NASA STEREO (Solar Terrestrial Relations Observatory) mission (see Report of the NASA Science Definition Team, <http://sd-www.jhuapl.edu/STEREO/>).

4. CORONAL MASS EJECTIONS

A major discovery, made through development of spaceborne coronagraphs in the early seventies of this century, was the detection of huge ejections of plasma in the Sun's outer atmosphere. The ejections had speeds of a few tens of km/s up to more than 2000 km/s, an average outward propelled mass of $\sim 10^{12}$ kg of solar material and an average width of $\sim 45^{\circ}$ heliolatitude. Figure 10 shows a spectacular example of a fast (~ 1600 km/s) CME observed by today's most sophisticated spaceborne white-light coronagraph LASCO (Large Angle and Spectrometric Coronagraph) on board SOHO.

After the discovery of CMEs, it was natural to think of a relationship to the observed transient disturbances in the

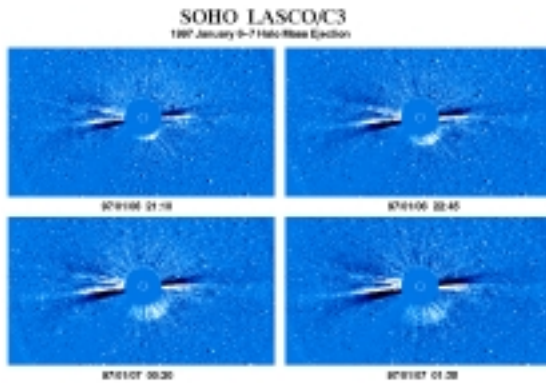


Figure 11. Development of a halo CME detected by SOHO/LASCO on January 6, 1997. The field of view is 4-30 R_s . Figure courtesy SOHO/LASCO consortium.

interplanetary medium. It is now well established, that CMEs are indeed the causes of transient interplanetary shocks and that the shocks are driven by the outward propelled solar material (Sheeley et al. 1985, Gosling 1990, Bothmer & Schwenn 1996, 1998). This is the reason why the transient solar wind streams are commonly referred to as “CMEs in the solar wind”. Note that there may likely be considerable evolution of the plasma and magnetic characteristics of CMEs on their way from the Sun into the heliosphere.

CMEs have now also been identified unambiguously as the sources of the strongest geomagnetic storms (Tsurutani et al. 1988; 1992, Gosling 1993, Bothmer & Schwenn 1995). Bothmer & Schwenn found, that, except one, all storms with $K_p \geq 8$ between 1966-1990 for which they could identify their interplanetary causes from near Earth satellite measurements, were caused by CMEs. The result was independent of the phase of the solar cycle so that just the frequency of geomagnetic storms of this magnitude varies, but not their origins. As an explanation for this finding, Bothmer & Schwenn (1995) concluded, that only CMEs can transport or cause, either through interaction with the ambient plasma (causing magnetic field compressions) or through their internal fields, sufficiently strong southward magnetic field components in the heliosphere. In this way, in coincidence with pronounced wind speeds, CMEs efficiently stimulate geomagnetic activity above a certain threshold.

CMEs are today considered as the prime triggers for space weather hazards rather than solar flares (Gosling 1993, Crooker 1994). The topic of the physics of CMEs and their interplanetary consequences still leaves a large number of open questions to be answered, e.g., which CMEs are geo-effective and which ones are not. Certainly, it seems to be the case that the fastest CMEs are nearly always associated with flares, but there are

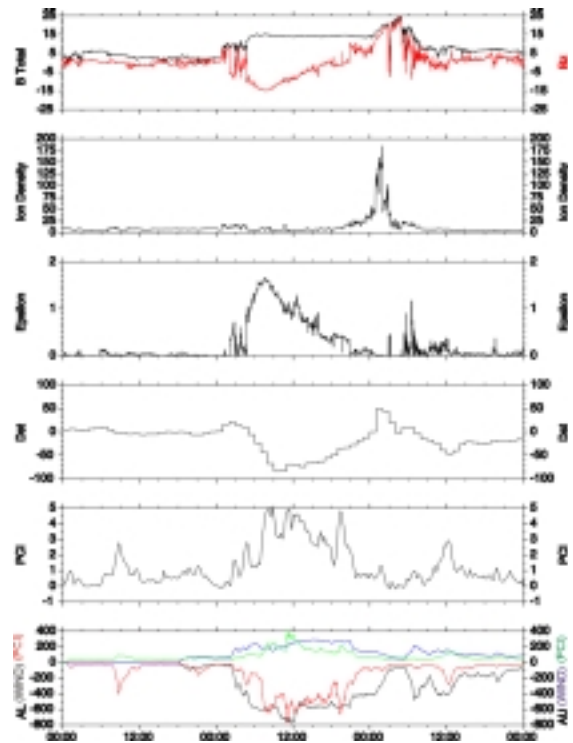


Figure 12. Geomagnetic and solar wind parameters for the January 6, 1997 halo CME that passed the Earth on January 10, 1997. Shown is the time interval from 00:00 UT on January 9 to 24:00 UT on January 11. Note the correlation between the peak southward component ($-B_z$) of the IMF and the maximum of geomagnetic activity. From Fox et al. (1998).

also other CMEs that are definitely not associated with flares, but are strongly geo-effective, and nonetheless accelerate particles to MeV energies (McAllister et al. 1996, Kahler et al. 1998). A recent example for such an event is the halo CME on January 6, 1997 (Figure 11), that propagated earthward (Burlaga et al. 1998). Figure 12 shows, that the CME caused a geomagnetic storm on January 10. It was a spectacular event in the media because the CME may have caused the malfunction of an AT&T telecommunication satellite (http://www-istp.gsfc.nasa.gov/istp/cloud_jan_97/). Halo CMEs are called those white-light coronagraph events which appear as bright “rings” in the telescope’s field of view, surrounding the occulter. They propagate towards/away from the observer and the brightness enhancements are seen once the disturbances expand in the field of view over the area of the coronagraph’s occulting disk that blocks out the sunlight from the visible solar disk. Since the Thompson-scattered white-light of the halo has maximum intensity perpendicular to the line-of-sight, contrary to limb CMEs, halo events are the ones hardest to detect and reliable measurements of their physical properties (speeds, densities, masses) are difficult to

determine. To observe earthward-directed CMEs, the ones one is naturally most interested in, in terms of space weather, a spacecraft needs to be positioned at a large ($> 40^\circ$) angle with respect to the Sun-Earth line (Schmidt & Bothmer 1996, <http://sd-www.jhuapl.edu/STEREO>).

Bothmer & Rust (1997) pointed out, that the internal magnetic field of the January 97 halo CME matched the one that was inferred from the solar magnetic field structure at the site of the associated filament, that disappeared within the CME's source region, under the assumption of magnetic helicity conservation. Thus, the internal field could have been predicted at times the CME was detected to leave the Sun (~ 4 days before arrival at Earth in the case of a CME with moderate speed). A very illustrative event proving the conclusions of Bothmer & Schwenn (1994), Bothmer & Rust (1997), Bothmer & Schwenn (1998) was observed on January 3, 1998 when a large polar crown filament disappeared in association with a CME (<http://www-istp.gsfc.nasa.gov/istp/events/1998jan3/>). The magnetic flux-rope CME passed the Earth on January 6 and its internal magnetic field structure agreed with the one expected from the magnetic field polarities at the

filament site (D. Webb, R. Lepping, priv. communications). These findings present a great step forward for space weather predictions since they show that magnetic fields within CMEs may become predictable from measurements of the solar magnetic field and simultaneous coronal observations.

5. SOLAR ENERGETIC PARTICLE EVENTS

Major solar energetic particle (SEP) events and galactic cosmic rays present a serious radiation risk for humans in space, e.g., on missions to Mars or Moon (Foundations of solar particle event risk management, Anser, Arlington, VA 22202, USA), and they can lead to severe satellite subsystem failures and even spacecraft/satellite losses through damage of solar arrays, surface materials and microprocessors (e.g., Baker et al. 1998, Lanzerotti et al. 1997). A recent example is the single event upset (SEU) in the Star Sensor Unit of the SOHO spacecraft through energetic particle radiation, which happened on February 14, 1999. The SEU led the spacecraft system run into an Emergency Sun Reacquisition (ESR) status that fortunately was resolved on February 18, 1999, when

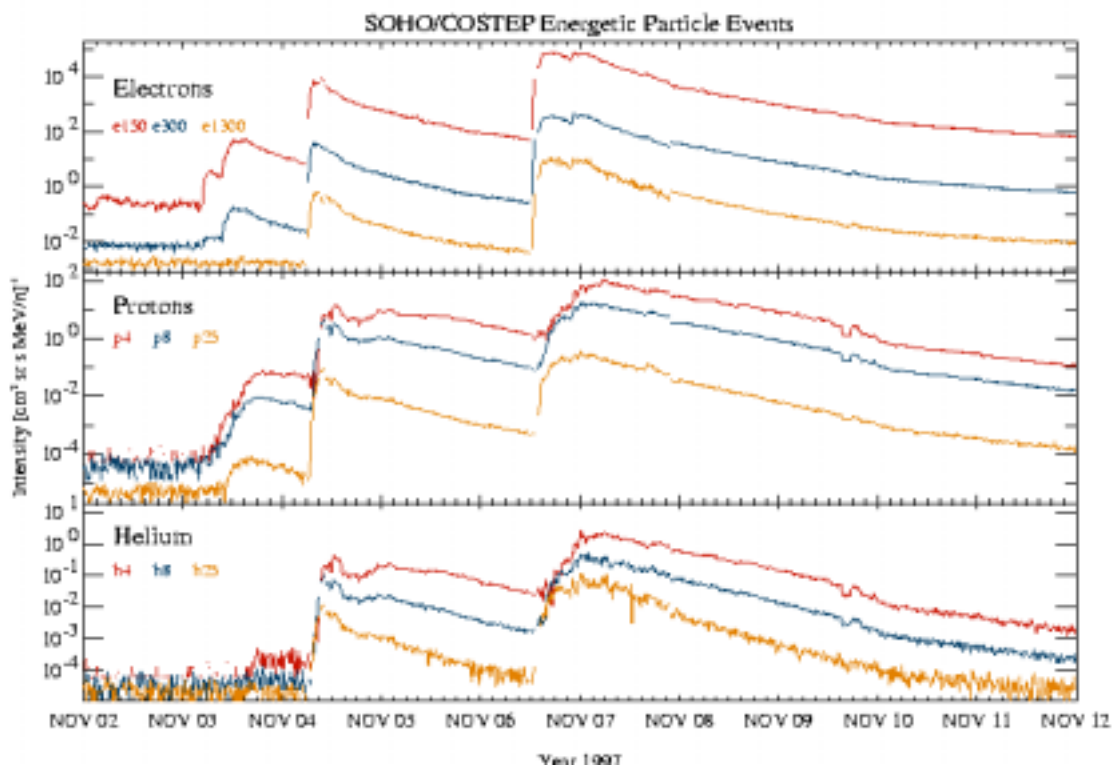


Figure 13. Major solar energetic particle events as measured by SOHO/COSTEP from November 2 - November 12, 1997. The parameters plotted in the individual panels are from top to bottom: 0.25-0.7 (top curve), 0.67-3.00, 2.64-6.18 MeV (bottom curve) electrons; 4.3-7.8 (top curve), 7.8-25.0, 25.0-40.9 (bottom curve) protons; 4.3-7.8 (top curve), 7.8-25.0, 25.0-40.9 (bottom curve) MeV/n ∇ -particles. Courtesy SOHO/COSTEP consortium.

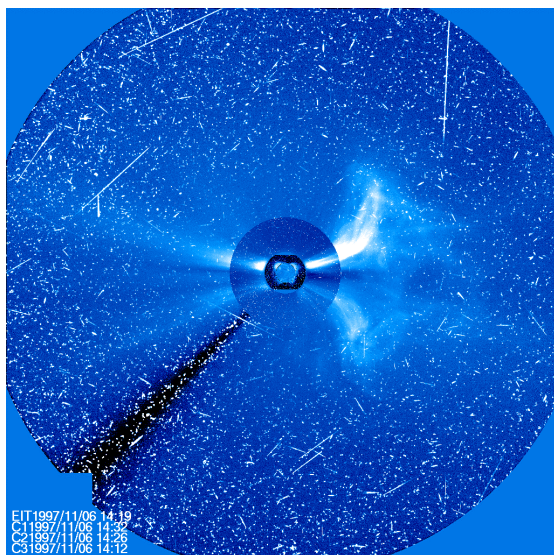


Figure 14. SOHO/LASCO CCD image of the November 6, 1997 west-limb CME. The speed of the CME was ~ 1600 km/s. The field of view is $2\text{-}30 R_s$. The bright dots and strikes in the image reflect impacts of solar energetic particles on the CCD. The strikes are presumably due to grazing incidence particles. It seems adequate to term such events energetic particle “blizzards” or proton “snowstorm”.
Courtesy SOHO/LASCO consortium.

SOHO went back to normal operations mode (<http://sohowww.estec.esa.nl/>). This event demonstrates directly the importance of SEP events in terms of space weather.

The first major particle events of solar cycle 23 were observed in November 1997. Figure 13 shows electron, proton and helium fluxes at MeV energies measured by the COSTEP (Comprehensive Suprathermal and Energetic Particle Analyzer) in these events. All the events were associated with CMEs detected by SOHO/

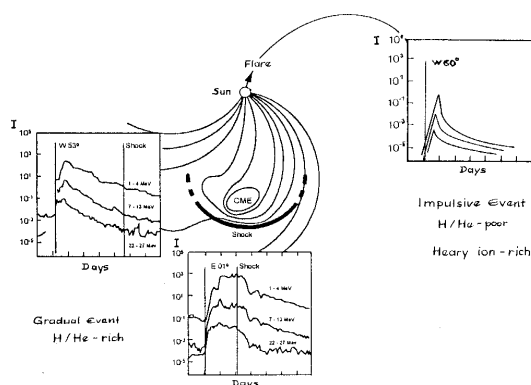


Figure 15. Intensity-time profiles for protons at different energies at two spacecraft (STEREO 1, 2), viewing a fast CME at different heliolongitudes. An impulsive, short-lived, flare associated SEP event is depicted to the right. Adapted from Reames (1994).

LASCO. The largest particle event, since start of the SOHO mission in December 1995, was measured on November 6 and was related to the onset of the fastest CME registered by SOHO/LASCO so far. The speed of the CME was about 1600 km/s (C. St. Cyr, priv. communications). Its onset time was about 11:50 UT on November 6, and the first $0.25\text{-}0.7$ MeV electrons were detected by COSTEP at $\sim 12:30$ UT. The scatter-free travel time along the IMF for a 0° pitch angle to 1 AU is about 11 minutes for 0.7 MeV electrons. The gradual intensity increase and the considerable time delay to the associated X-ray flare at 11:49-12:01 UT, at S18W63, are in favour for the assumption that the particles have been accelerated by a shock wave caused by the CME that presumably expanded to the magnetic field lines that connected SOHO with the Sun’s western hemisphere. Figure 14 beautifully visualises the impact of energetic particles at SOHO during this event, most likely protons with energies >50 MeV, visible as bright dots and strikes in the LASCO CCD image. The strikes are presumably due to grazing incidence particles. It seems adequate to term such events energetic particle “blizzards” or proton “snowstorm”.

Recently it has become obvious from the analysis of SEP events measured in the interplanetary medium and simultaneous optical observations, that CMEs and not flares are the prime sources of major intensity increases of accelerated particles, and that the observed intensities and spectra depend on the observer’s position with respect to the center of the CME (Cane et al. 1987, Reames 1994, Kahler 1994, Bothmer et al. 1997). Kahler et al. (1998) have shown that protons > 30 MeV and electrons > 1 MeV have been accelerated by CMEs that were unambiguously not associated with flares. One now distinguishes basically between two types of SEP events: Impulsive events of flare origin with time durations of several hours, which are electron-, $^3\text{He}/^4\text{He}$ - and heavy ion (e.g., Ne, Fe, Mg)-rich, with H/He ratios of ~ 10 , and gradual events with higher intensities and time durations at the order of days, which are electron poor, without ^3He abundances and heavy ions, with H/He ratios of ~ 100 (e.g., Reames 1994). Gradual events, which are of long duration and high intensity, are thought to be accelerated at shocks driven by fast CMEs (Reames et al. 1996). Due to the high long-lasting particle fluxes, gradual SEP events are the most important ones in terms of radiation hazards.

Figure 15 shows the basic two types of SEP events and the different intensity time profiles for particles at different energies observed by two spacecraft, which are located at different positions with respect to the center of the CME. Note that energetic particles are observed once the shock reaches magnetic field lines that connect the spacecraft with the Sun. Compression is expected to be strongest at the western front of the CME’s leading edge so that particle acceleration should be most

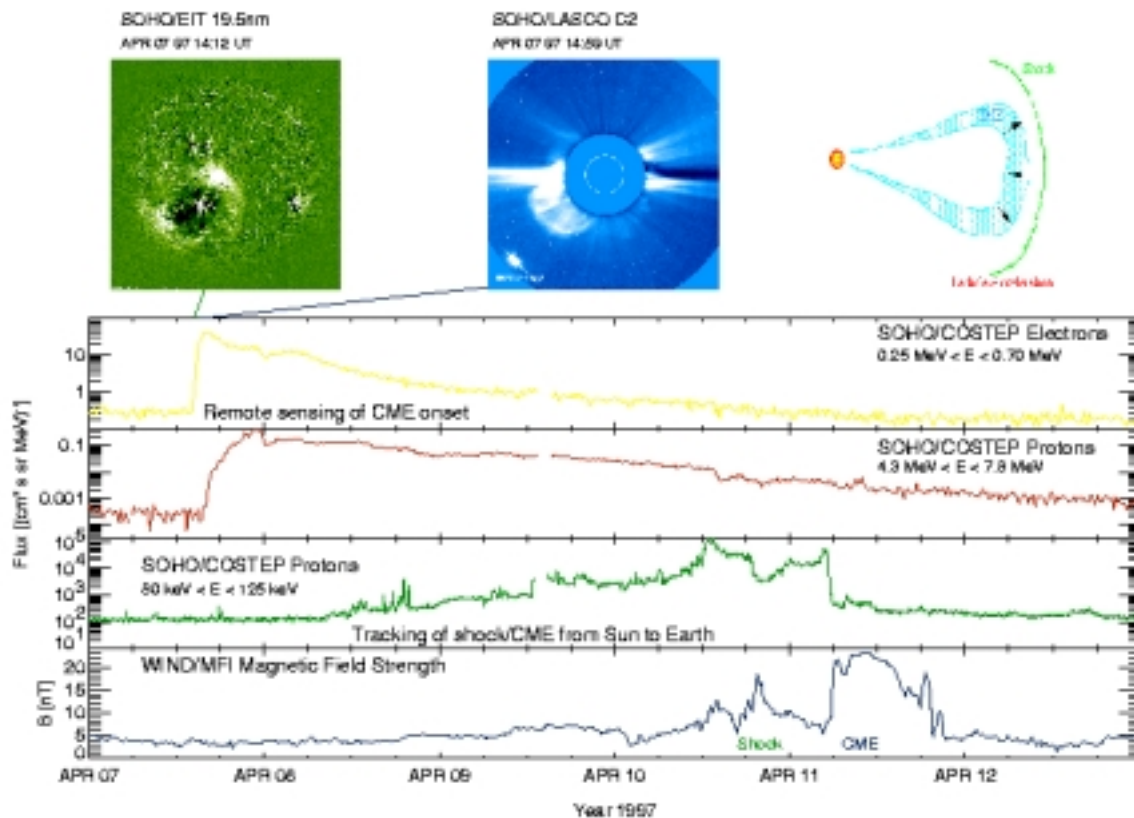


Figure 16. SOHO/EIT/LASCO/COSTEP EUV, white-light, electron, and proton measurements for a halo CME on April 7, 1997. EUV observations show the associated coronal wave, white-light observations the halo CME. A sketch to the upper right depicts the outward propagating CME and its shock. From Bothmer et al. 1997.

effective in this region. Further, particle acceleration is certainly most efficient close ($<10 R_S$) to the Sun, where the CME is fastest and is most strongly interacting with the ambient corona and solar wind, and where the plasma density and magnetic field strength is high. Particles of MeV energies typically show an intensity maximum within minutes to hours after the onset of the solar event in cases the observer is magnetically well connected to the source (east-limb events are less favourable). This view is represented by Figure 16 showing measurements of MeV protons and electrons and keV protons for a halo CME in April 1997 (Bothmer et al. 1997). Particles at higher energies provide information about the onset of the event, in this case the first electrons arrived at SOHO at $\sim 14:20$ UT on April 7, 1997, about half an hour after the onset of the CME. Contrary to the MeV particles, the intensity of 80-125 keV protons starts to rise above instrument background levels at $\sim 09:00$ UT on April 8. The peak intensities occur later, in coincidence with the shock and CME passage at Earth on April 10/11. Protons at keV may thus be used as early indicators for earthward-directed halo CMEs driving a shock wave ahead. The prediction of MeV fluxes at the onset of solar events

remains a hard problem, that will presumably require a better understanding of CME onset mechanisms and the evolution of active regions and the solar magnetic field in general.

6. OUTLOOK

After reviewing briefly some of the major important aspects of the physics of the solar corona and solar wind, and that of solar energetic particle events, I think it is adequate to conclude that the major breakthroughs of space science obtained during the past years have led to a new level of understanding in solar-terrestrial physics. This level seems to be far more improved than that of, e.g., the first pioneers of Earth weather prediction models. Solar and interplanetary observations taken by a moderate fleet of monitoring satellites and further improved theoretical models should help establish the first realistic space weather predictions early in the new millennium. A precise quantitative prediction of the conditions at geospace still needs an enhanced understanding of the evolution and modulation of the solar output in the interplanetary

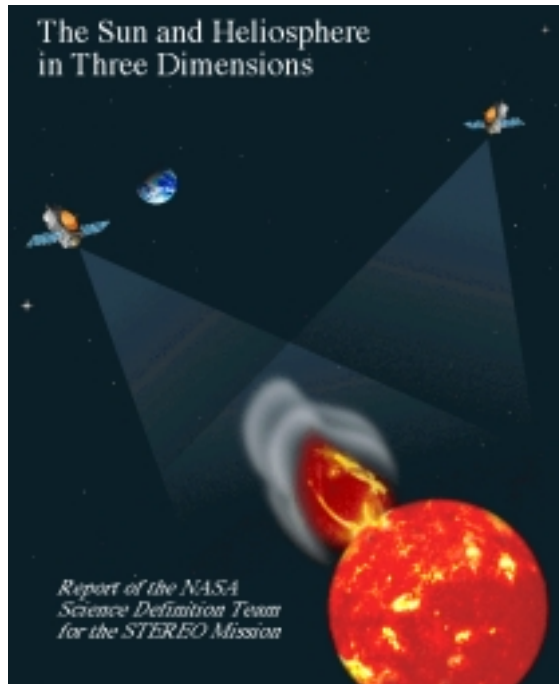


Figure 17. Sketch of NASA's solar STEREO mission. Courtesy NASA STEREO Science Definition Team (<http://sd-www.jhuapl.edu/STEREO/>).

medium. These scientific objective will hopefully be developed within the next years. The NASA solar STEREO (Solar TERrestrial Relations Observatory) mission (Figure 17) consists of two suitable equipped spacecraft, that will obtain simultaneous solar/heliospheric observations at positions away from the Sun-Earth line. STEREO, which is scheduled for launch in 2004, will study directly for the first time, amongst other objectives, Earth-directed solar eruptions. The mission will represent a new milestone in terms of space weather predictions.

ACKNOWLEDGMENTS

This research was supported by DLR (Deutsches Zentrum für Luft- und Raumfahrt) under the SOHO project. The author thanks A. Posner, N. Fox and K. Ivory for providing Figures for this paper and the conference organizers for inviting him to this conference. The author is especially grateful for Norma Crosby's patience in awaiting this paper and for many helpful comments.

REFERENCES

Allen, J., Sauer, H., Frank, L. et al. 1989, EOS Trans. AGU, 70, 1479
 Baker, D.N., Allen, J.H., Kanekal, S.G. et al. 1998, EOS Trans. AGU, 79, 40, 477
 Bothmer, V., Schwenn, R. 1998, Ann. Geophysicae, 16, 1
 Bothmer, V., Rust, D.M. 1997, AGU Geophys. Monogr. 99, 139
 Bothmer, V., Schwenn, R. 1996, Adv. Space Res., 17, 319
 Bothmer, V., Schwenn, R. 1995, J. Geomag. Geoelectr., 47, 1127

Bothmer, V., Schwenn, R. 1994, Space Sci. Rev., 70, 215
 Bothmer, V., Posner, A., Kunow, H. et al. 1997, ESA SP-415, 207
 Burlaga, L.F., Fitzenreiter, R., Lepping, R. et al. 1998, J. Geophys. Res., 103, 277
 Burlaga, L.F., Klein, L., Sheeley, N.R. et al. 1982, Geophys. Res. Lett., 9, 1317
 Cane, H.V., Sheeley, N.R., Howard, R.A. 1987, J. Geophys. Res., 92, 9869
 Crooker, N. 1994, Nature, 367, 595
 Crooker, N., Lazarus, A.J., Lepping, R.P. et al. 1996, Geophys. Res. Lett., 23, 10, 1275
 Eddy, J.A. 1979, NASA Solar Phys., Washington, D.C., 402
 Fisk, L.A. 1996, J. Geophys. Res., 101, 15547
 Fox, N.J., Peredo, M., Thompson, B.J. 1998, Geophys. Res. Lett., 25, 2461
 Gorney, D.J. 1990, AGU Rev. of Geophys., 28, 315
 Gosling, J.T. 1993, Phys. Fluids B-5, 7, 2638
 Gosling, J.T. 1993, J. Geophys. Res., 98, 18937
 Gosling, J.T. 1990, AGU Geophys. Monogr. 99, 1
 Gosling, J.T., Bame, S.J., McComas, D.J. 1995, Space Sci. Rev., 72, 99
 Gosling, J.T., Bame, S.J., Feldman, W.C. 1995, Geophys. Res. Lett., 22, 1753
 Gosling, J.T., Pizzo, V., Bame, S.J. 1973, J. Geophys. Res., 78, 2001
 Hirshberg, J., Bame, S.J., Robbins, D.E. 1972, Sol. Phys., 23, 467
 Kahler, S.W. 1994, Astrophys. J., 428, 837
 Kahler, S.W., Cane, H.V., Kurt, V.G. et al. 1998, J. Geophys. Res., 103, 12069
 Lanzerotti, L.J., Thomson, D.J., MacLennan, C.G. 1997, Bell Labs Technical J., 5
 Marsden, R.G., Smith, E.J. 1997, Adv. Space Res., 19, (6)825
 McAllister, A.H., Dryer, M., McIntosh, P. et al. 1996, J. Geophys. Res., 94, 9995
 McComas, D.J., Bame, S.J., Barraclough, B.L. et al. 1998, Geophys. Res. Lett., 25 (1), 1
 McKibben, R.B., Connell, J.J., Lopate, C. et al. 1995, Space Sci. Rev., 72, 367
 Reames, D.V. 1994, ESA SP-373, 107
 Reames, D.V., Barbier, L.M., Ng, C.K. 1996, Astrophys. J., 466, 473
 Russell, C.T., McPherron, R.L. 1973, Space Sci. Rev., 15, 205
 Schmidt, W.K.H., Bothmer, V. 1996, Adv. Space Res., 17, 369
 Schwenn, R. 1990, in Physics of the Inner Heliosphere, Springer-Verlag Berlin Heidelberg, 99
 Shea, M.A., Smart, D.F., Allen, J.H. et al. 1992, IEEE Trans. of Nuclear Sci. 39, 6, 1754
 Sheeley, N.R., Howard, R.A., Koomen, M.J. et al. 1985, J. Geophys. Res. Lett., 90, 163
 Tsurutani, B.T., Gonzalez, W.D., Tang, F. et al. 1992, Geophys. Res. Lett., 19, 1, 73
 Tsurutani, B.T., Gonzalez, W.D., Tang, F. et al. 1988, J. Geophys. Res., 93, 8519
 Wang, Y.-M. 1994, Astrophys. J., 437:L67
 Wang, Y.-M., Sheeley, N.R., Walters J.H. et al. 1998, Astrophys. J., 498:L165
 Wang, Y.-M., Sheeley, N.R., Phillips, J.L. et al. 1997, Astrophys. J., 488:L51
 Wang, Y.-M., Hawley, S.H., Sheeley, N.R. 1996, Science, Vol. 271, 464